Frontiers in Heat and Mass Transfer (FHMT), 5, 1 (2014)
DOI: 10.5098/hmt.5.1

Global Digital Central
ISSN: 2151-8629

Frontiers in Heat and Mass Transfer

Available at www.ThermalFluidsCentral.org

SINTERING OF TITANIUM AND NICKEL NANOPOWDERS WITH A ND:YAG NANOSECOND LASER

Jing Huang, Vitaly E. Gruzdev, Yuwen Zhang*, and J. K. Chen

Department of Mechanical and Aerospace Engineering, University of Missouri, Columbia MO 65211, USA

ABSTRACT

Experimental study on laser sintering of nanosized titanium and nickel powders using a nanosecond laser is reported in this paper. Pulse laser with a wavelength of 532 nm and pulse width (FWHM) of 23 nanoseconds is used. The diameters of the metal nanoparticles are between 35 to 50 nanometers. Pulse repetition rates range between 100 and 10,000 Hz and the average power is from 1 to 20 W. The powder bed is placed on a moving stage to control the scanning velocity. Sintered metal strips with 20 mm length are formed by focusing the laser beam on the surface of the moving power bed. Experiment results discover four different patterns of sintered metal strips. Nickel powder shows poor sintering ability due to severe shrinkage of the powder bed, while titanium powder forms solid sintered strips under specific parameters. However, scaly structure is observed in certain conditions which weakens the mechanical strength of the sintered strips.

Keywords: Laser Sintering; Nanopowder; Nanosecond laser.

1. INTRODUCTION

Since it was introduced in mid 1980s for the first time, theoretical and experimental studies on selective laser sintering (SLS) have been studied both theoretically and experimentally in a large number of reported works (Agarwala *et al.*, 1995; Kruth *et al.*, 2004, 2007; Peltola *et al.*, 2008; Wang *et al.*, 2006; Chen and Zhang, 2007; Xiao and Zhang, 2007; Shi and Zhang, 2008). The researchers developed various methods to improve the original idea of building working parts layer by layer through laser sintering of fine material particles. Various fabrication parameters were tested thoroughly, including laser wavelengths, intensity, laser beam size, scanning strategy, and so on. Different materials were used, single-component or mixture. The quality and efficiency of the technology has been improved significantly since then. Some commercial systems are also available now in the market.

One of the most attractive advantages of SLS is its ability to process a wide range of material: polymers, metals, ceramics, etc. (Kruth *et al.*, 2003). However, the mostly investigated materials in SLS are still commercially available metal powders, such as tool steel, titanium, etc. (Kruth *et al.*, 2007; Childs *et al.*, 2003; Fischer *at al.*, 2003). Fischer at al. (2003; 2004a,b; 2005a,b) carried out a large amount of works on the sintering of single phase metal powders. Their work showed that by optimizing the laser parameters, the degree of porosity, density and the microstructure of the finished work piece could be controlled. Some others used a combination of two different kinds of powders, or coated powder (such as nylon-coated or polymer coated metal particles) to achieve sintering of high melting point metal at a relatively low temperature (Zhang *et al.*, 2000; Kruth *et al.*, 2005).

Selective laser sintering was also applied in tissue engineering in which scaffolds fabricated in high precision plays an important role. Chua *et al.* reported to use SLS technology to process a biocomposite blend comprising of polyvinyl alcohol and hydroxyapatite and create scaffolds aiming at dealing with craniofacial and join defects (Chua *et al.*, 2004). Ciardelli *et al.* (2005) studied the influence of laser beam parameters, including beam scanning speed and power on the sintering of bioartificial blends of poly-ε-caprolactone and polysaccharide. The materials used in these works were mostly synthetic in considering the special requirement of biomedical issues such as degradability, biocompatibility, non-immunogenicity, etc. (Tang *et al.*, 2003).

In the aforementioned works, most were conducted with conventional metal powder, where the dimensions of size are in micrometers or larger. Recently researchers started to study the nano-liquid phase laser sintering of metal powder which aimed at developing the next generation large scale integrated circuit printing technology. Ko *et al.* (2007) reported their work on laser sintering of inkjet-printed metal nanoparticles. The advantage of high precision of SLS was fully utilized to achieve high resolution patterning which was crucial for the large-area, flexible electronics manufacturing. The heat affected zone and thermal damage to the substrate was well controlled to enhance the resolution.

As the basis of nanotechnology, nanopowders are consisted of solid particles that measured on the nanoscale, only the size of three to five molecules together. Because of the size, they showed many unique characteristics that are different from the materials in bulk size. An example is the self-heating of aluminium nanopowder with liquid water which can be utilized to produce hydrogen (Astankova *et al.*, 2008).

Another imporant factor in SLS technology is the laser. In most studies, continuous wave lasers were used because they are more mature and have the advantage of low cost. With the development of ultrafast laser, nanosecond, even femtosecond laser are more and more reliable and affordable. As pointed out by R. Glardon, *et. al*, nanosecond laser offers a wider range of control and better dimension accuracy than continuous wave lasers which are important for high precision SLS (Glardon *et al.*, 2001).

In this paper, we will report our experimental work on laser sintering of solid phase nanopowders. Titanium and Nickel

* Corresponding author. Email: zhangyu@missouri.edu

Global Digital Central
ISSN: 2151-8629

nanopowders and their mixture (1:1 volume ratio) were tested. A Nd-YAG nano-second laser was used to form sintered metal strips on the surface of the powder bed. Average laser power, pulse repetition rate and powder bed moving speed were changed to find their influence on the quality of the final pieces.

2. EXPERIMENTAL SETUP AND PROCEDURES

A nanosecond Nd:YAG laser from Clark-MXR is used in the experiments. The laser had the wavelength of 532 nm and pulse width (FWHM) of 23 nanoseconds. The repetition rate of laser pulses was adjustable between 10^2 and 10^4 Hz, and the average power was adjustable between 1 and 20W (depending on frequency.)

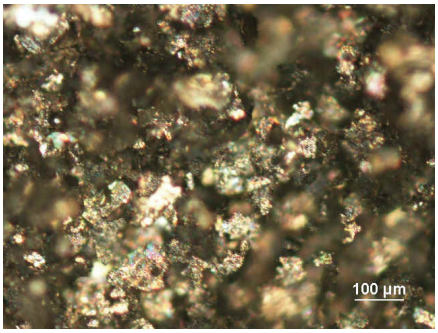

(a) Optical microscope

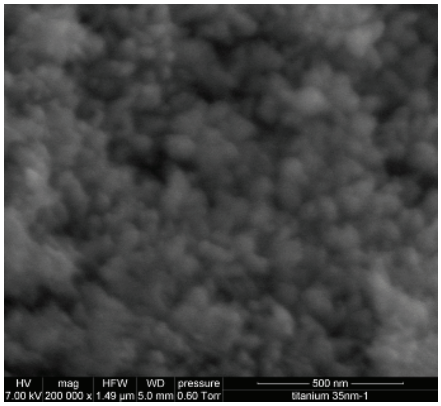

(b) SEM

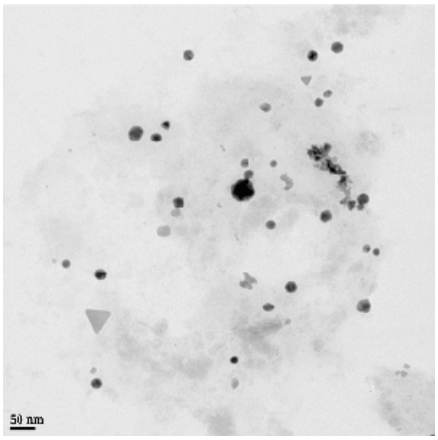

(c) TEM

Fig. 1 Titanium powder under different magnification factor

The nanopowder was provided by Nanostructured & Amorphous Materials. Two different materials were used: Ti (99%) and Ni (99.7%). The average size of the particles ranged from 30 to 50 nanometers. The titanium powders were characterized by optical microscope, transmission electron microscope (JEOL 1400) and scanning electron microscope (Hitachi S-4700). Figure 1 shows the pictures of the titanium powder under different amplification factors. Due to the high flammability of nickel powder in air, we did not observe it under microscopes. The average densities of powders were 1.114 g/mL and 0.872 g/mL for the titanium and nickel powder, in comparison to 4.506 g/cm^3 and 8.908 g/cm^3 of bulk values, respectively. This means the nickel power has a much higher porosity than the titanium powder.

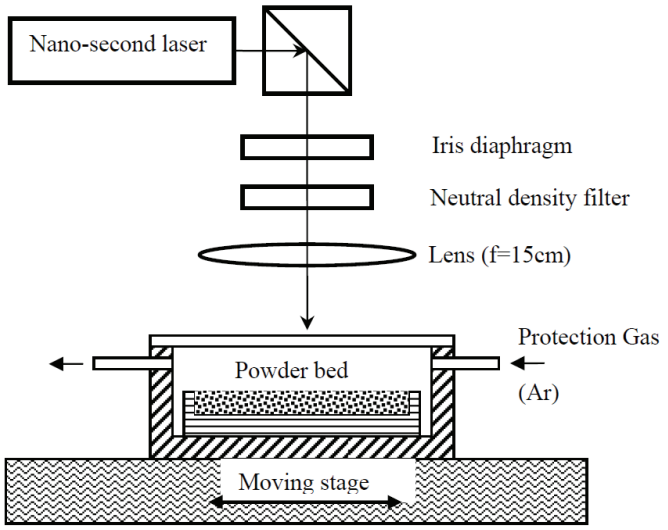

Fig. 2 Experiment platform and optical path

Figure 2 shows the schematic diagram of the test platform. Neutral density filters with different optical densities were used to change the average power without changing other parameters. Power density of the laser pulse train was measured with a pyroelectric energy sensor prior to each test. The distance between lens and powder bed surface was kept at a constant to maintain a laser beam diameter of 0.3 mm on the powder bed surface. The ceramic powder bed was placed in a cylindrical chamber with glass cover on the top. The chamber was infused with argon gas to prevent oxidation at high temperature. The whole chamber was placed on a moving stage that can be controlled by a computer to achieve different scanning speed. The parameters used in the experiment are listed in Table 1.

Table 1 Parameter range used in the experiment

Powder	Repetition rate (Hz)	Average power (W)	Moving speed (cm/s)
Nickel	700 - 5000	1.033 – 15.76	0.2 – 0.8
Titanium	1100 - 3000	3.51 – 13.63	0.2 – 1.0
Nickel + Titanium	3000	1.691 – 13.14	0.2 – 1.5

Before the experiments described below we conducted some tests with fixed single point of laser irradiation. The purposes of these tests were to find an appropriate range of laser parameters, protection gas flow rate, optical path adjustment steps and experiment procedures.

3. RESULTS AND DISCUSSIONS

3.1 Nickel powder

Fig. 3 Typical result by sintering nickel nanopowder

The nickel powder showed serious powder shrinkage during sintering under the above parameter ranges. Figure 3 shows a typical

Global Digital Central
ISSN: 2151-8629

result, with the average power of 3.5 W, repetition rate 1500 Hz and scanning speed of 0.2 mm/s. The circles in the figure showed some nickel droplets caused by balling effects during the irradiation, with diameters around 1 mm. With such a problem, no usable working piece could be formed. The shrinkage of the powder bed was due to a relatively low powder density. As stated in section 2, the porosity of nickel powder is much smaller than titanium powder, which caused a more loose structure in the powder bed.

3.2 Titanium powder

The effect of laser power, repetition rate and scanning speed was tested by keeping all the other parameters constant while changing one of the parameter mentioned in the preceding subsection. Figure 4 shows the results with different average powers, while the repetition rate and scanning speed were kept at 3000 Hz and 0.2 mm/s, respectively. Since the aim of current work is to find the parameter range for further study, a simple strip pattern was chosen instead of a raster scanned area pattern. The strip length was kept constant at 20 mm. It can be seen that with higher laser power, the strip width increased because higher temperature led to further heat transfer.

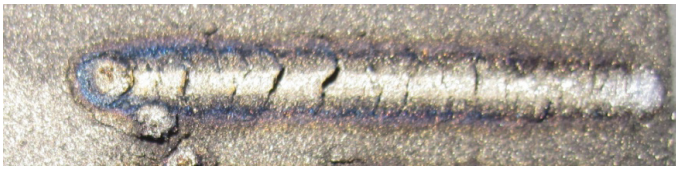

(a) Average power 6.7 W

(b) Average power 8.5 W

(c) Average power 13.6 W

Fig. 4 Metal strip formed with titanium powder under different laser power (Scanning speed is 0.2 mm/s, and repetition rate is 3000 Hz)

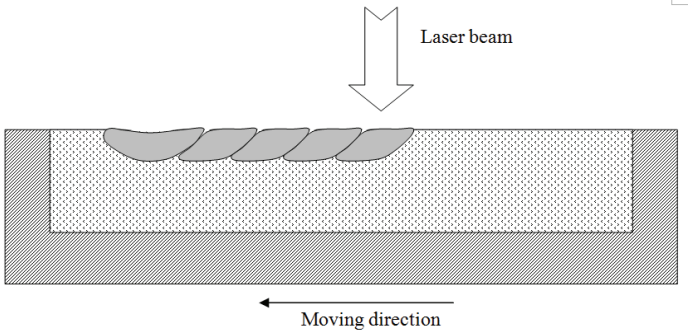

Fig. 5 Formation of a scale structure

The pictures showed that only power in a narrow range (Fig. 4b) would form ideal metal strip. When the laser power is too high or too low (Fig. 4a, 4c), a scaly interlayer structure would be formed. The mechanical strength of this structure was very poor as the strips were prone to breakage. Compared to the results reported in Fischer *et al.* (2003), which used titanium particles with the size of micrometer level, this optimum power density to achieve smooth flattened surface is about in the same range.

The process to cause the scale struture was analyzed based on the understanding of the sintering process. As shown in Fig. 5, when new melting pool took into being with the moving of the powder bed, melted metal fluid would flow under the old, already half-solidified melting pool. Then the continuous scanning of the laser beam would cause this scaly interlayer structure. Only in an appropriate combination of solidification time, which was related to laser power and moving speed, this effect would be alleviated to a low level.

Figure 6 shows the effect of moving speed of the powder bed, i.e., the scanning speed. It showed similar tendency as Fig. 5, only at a specific speed, the strip showed smooth appearance. In other cases, the scale structure would form and caused bad mechanical strength of the formed strips. At low scanning speed, each point on the power bed received more laser irradiation, thus the resolidification process became longer. As explained above, the heavier melted metal flew to the deeper part of the powder bed and formed scale structure and led to weak structure strength. When the scanning speed was too high, the metal particles received not enough energy to melt and sinter together appropriately. This is especially severe for the particles far away from the laser path because the energy received by these regions is not directly from the laser irradiation but from the heat transfer through the powder bed. As shown by the work of Xu *et.al*. (2007), the thermal conductivity of metal nanoparticle bed can be four orders of magnitude lower than that of bulk metal. This effect can be seen clearly in Fig. 6 (c) and (d). Different sintering regimes can be between these two limits and other parameters also influenced this balance, such as particle size and pulse frequency.

(a) Scanning speed 0.4 mm/s

(b) Scanning speed 0.6 mm/s

(c) Scanning speed 0.8 mm/s

(d) Scanning speed 1.5 mm/s

Fig. 6 The metal strip formed with titanium powder under different scanning speed (average power is 9.4 W, and the repetition rate 3000 Hz)

Different pulse frequencies (1000 Hz ~ 4000 Hz) were tested in the experiment to see its effect. However, the frequency range was not very wide because it was difficult to keep a constant average power while changing repetition rate. The experiment results showed little difference in the pulse frequency tested. This was because the intervals between two single pulses ranged from 0.25 to 1 ms, which were always several magnitudes larger than the duration of each single pulse

(23ns).

In addition to the above results, in the experiments we found that the quality of powder bed influenced sintering results significantly. The powder bed must be well vibrated to form a solid and smooth surface to ensure the repeatability of the experiment results. Although every effort has been taken to achieve best smoothness of the powder bed, the toughness of the bed surface cannot be compared to the size of individual particles.

3.3 Titanium/Nickel mixture

Finally, the titanium/nickel powder mixtures were tested. The powders were mixed with a volume ratio of 1:1. The results were similar to pure nickel powder, only some unconsolidated structures were formed. Figure 7 shows a typical result (Average power 5.4 W, scanning speed 0.1 mm/s, repetition rate 3000 Hz). More experiments are needed to find an appropriate mixing ratio of titanium and nickel nanopowders.

Fig. 7 Sintering result of titanium/nickel mixture (average power is 5.4 W, scanning speed is 0.1 mm/s, and repetition rate is 3000 Hz)

By comparing all the experiment results, we can summarize the formed pieces into 4 different sintered strip patterns: (A) Scale structure, such as shown in Fig. 4(b); (B) Well sintered, such as shown in Fig. 4(a); (C) Balling structure, such as shown in Fig. 3; (D) Porous structure as shown in Fig. (7). The corresponding parameters and resulting patterns are summarized in table 2. It is showed that in order to get a good sintered strip, the parameters should be sought under the following range: average power 5~8 W, repetition rate about 3000Hz, scanning speed 0.2~0.5 mm/s. However, it is also clear that there is still a lot blank area of parameters left unstudied in this table, which will be our work in the next step.

Table 2 Summary of experiment results in four patterns

Frequency (Hz)	Average Power (W)	Scanning Speed (mm/s)	Pattern
3000	0.2	13.63	A
3000	0.2	10.62	A
3000	0.2	9.64	A
3000	0.2	8.52	B
3000	0.2	6.78	B
3000	0.2	5.42	A
3000	0.2	3.51	D
3000	0.2	1.718	D
3000	0.1	9.61	A
3000	0.3	9.64	A
3000	0.4	9.63	A
3000	0.6	9.63	B
3000	0.8	9.61	B
3000	1.0	9.57	A
3000	1.5	9.6	A
3000	2.0	9.6	A
1300	0.2	5.44	D
1800	0.2	5.44	D
2300	0.2	5.42	D
4200	0.2	5.46	D
3500	0.2	5.41	D
3000	0.2	5.45	D
2000	0.2	5.44	D
1100	0.2	5.42	D

4. CONCLUSIONS

A nanosecond Nd-YAG pulsed laser was used to sinter titanium, nickel and their mixture nanopowders. Different laser powers, repetition rates, scanning speeds were used to study their influence on the metal strip formed by laser irradiation. By summarizing the experimental results, we can reach the following conclusions:

(1) For nickel powders, because of serious powder shrinkage after melting, there were no usable metal strips formed during the irradiation. It should be pointed out that the values of repetition rate and scanning speed between two tests are not very close in our experiments. We cannot completely rule out the possibility that better sintering results could be achieved in a very narrow range of parameters.

(2) For titanium powder, only a fine combination of laser power and scanning speed would lead to good quality of sintered strip. In other cases, scaly interlayer structure is obtained because of interaction between newly melted powder and resolidified pool. In the range we tested, pulse repetition rate showed little influence on the final results.

(3) With a volume ratio of 1:1, titanium/nickel mixture did not show a better property than pure titanium powder.

ACKNOWLEDGEMENTS

Support for this work by the U.S. National Science Foundation under Grant No. CBET-1066917 is gratefully acknowledged.

REFERENCES

Agarwala, M., Bourell, D., Beaman, J., Marcus, H., and Barlow, J., 1995, "Direct Selective Laser Sintering of Metals," *Rapid Prototyping Journal*, **1**(1), pp. 26-36.
http://dx.doi.org/10.1108/13552549510078113

Astankova, A.P., Godymchuk, A.Y., Gromov, A.A., and Il'In, A.P., 2008, "The Kinetics of Self-heating in the Reaction Between Aluminum Nanopowder and Liquid Water," *Russian Journal of Physical Chemistry A*, **82**(11), pp. 1913-1920.
http://dx.doi.org/10.1134/S0036024408110204

Chen, T., and Zhang, Y., 2007, "Thermal Modeling of Laser Sintering of Two-Component Metal Powder on Top of Sintered Layers via Multi-line Scanning," *Applied Physics A: Materials Science & Processing,* **86**(2), 213-220.
http://dx.doi.org/10.1007/s00339-006-3739-1

Childs, T.H.G., Hauser, G., and Badrossamay, M., 2005, "Selective Laser Sintering (Melting) of Stainless and Tool Steel Powders: Experiments and Modelling," *Proceedings of the Institution of Mechanical Engineers, Part B: Journal of Engineering Manufacture*, **219**(4), pp. 339-357.
http://dx.doi.org/10.1243/095440505X8109

Chua, C.K., Leong, K.F., Tan, K.H., Wiria, F.E., and Cheah, C.M., 2004, "Development of Tissue Scaffolds Using Selective Laser Sintering of Polyvinyl Alcohol/Hydroxyapatite Biocomposite for Craniofacial and Joint Defects," *Journal of Materials Science: Materials in Medicine*, **15**(10), pp. 1113-1121.
http://dx.doi.org/10.1023/B:JMSM.0000046393.81449.a5

Ciardelli, G., Chiono, V., Vozzi, G., Pracella, M., Ahluwalia, A., Barbani, N., Cristallini, C., and Giusti, P., 2005, "Blends of Poly-(ε-caprolactone) and Polysaccharides in Tissue Engineering Applications," *Biomacromolecules*, **6**(4), pp. 1961-1976.
http://dx.doi.org/10.1021/bm0500805

Fischer, P., Blatter, A., Romano, V., and Weber, H.P., 2005a, "Selective Laser Sintering of Amorphous Metal Powder," *Applied Physics A: Materials Science and Processing*, **80**(3), pp. 489-492.
http://dx.doi.org/10.1007/s00339-004-3062-7

Fischer, P., Leber, H., Romano, V., Weber, H.P., Karapatis, N.P., André, C., and Glardon, R., 2004a, "Microstructure of Near-Infrared Pulsed Laser Sintered Titanium Samples," *Applied Physics A: Materials Science and Processing*, **78**(8), pp. 1219-1227.
http://dx.doi.org/10.1007/s00339-003-2205-6

Fischer, P., Romano, V., Blatter, A., and Weber, H.P., 2005b, "Highly Precise Pulsed Selective Laser Sintering of Metallic Powders," *Laser Physics Letters*, **2**(1), pp. 48-55.
http://dx.doi.org/10.1002/lapl.200410118

Fischer, P., Romano, V., Weber, H.P., Karapatis, N.P., Boillat, E., and Glardon, R., 2003, "Sintering of Commercially Pure Titanium Powder with a Nd:YAG Laser Source," *Acta Materialia*, **51**(6), pp. 1651-1662.
http://dx.doi.org/10.1016/S1359-6454(02)00567-0

Fischer, P., Romano, V., Weber, H.P., and Kolossov, S., 2004b, "Pulsed Laser Sintering of Metallic Powders," *Thin Solid Films*, **453-454**, pp. 139-144.
http://dx.doi.org/10.1016/j.tsf.2003.11.152

Glardon, R., Karapatis, N.P., and Romano, V., Levy, G.N., 2001, "Influence of Nd:YAG Parameters on the Selective Laser Sintering of Metallic Powders," *CIRP Annals - Manufacturing Technology*, **50**(1), pp. 133-136.
http://dx.doi.org/10.1016/S0007-8506(07)62088-5

Ko, S.H., Pan, H., Grigoropoulos, C.P., Luscombe, C.K., Fréchet, J.M.J., and Poulikakos, D., 2007, "All-Inkjet-Printed Flexible Electronics Fabrication on A Polymer Substrate by Low-temperature High-Resolution Selective Laser Sintering of Metal Nanoparticles," *Nanotechnology*, **18**(34), 345202.
http://dx.doi.org/10.1088/0957-4484/18/34/345202

Kruth, J.P., Froyen, L., Van Vaerenbergh, J., Mercelis, P., Rombouts, M., and Lauwers, B., 2004, "Selective Laser Melting of Iron-Based Powder," *Journal of Materials Processing Technology*, **149**(1-3), pp. 616-622.
http://dx.doi.org/10.1016/j.jmatprotec.2003.11.051

Kruth, J.P., Levy, G., Klocke, F., and Childs, T. H. C., 2007, "Consolidation Phenomena in Laser and Powder-Bed Based Layered Manufacturing," *CIRP Annals - Manufacturing Technology*, **56**(2), pp. 730-759.
http://dx.doi.org/10.1016/j.cirp.2007.10.004

Kruth, J.P., Mercelis, P., Van Vaerenbergh, J., Froyen, L., and Rombouts, M., 2005, "Binding Mechanisms in Selective Laser Sintering and Selective Laser Melting," *Rapid Prototyping Journal*, **11**(1), pp. 26-36.
http://dx.doi.org/10.1108/13552540510573365

Kruth, J.P., Wang, X., Laoui, T., and Froyen, L., 2003, "Lasers and Materials in Selective Laser Sintering," *Assembly Automation*, **23**(4), pp. 357-371.
http://dx.doi.org/10.1108/01445150310698652

Peltola, S.M., Grijpma, D.W. Melchels, F.P.W., and Kellomäki, M., 2008, "A Review of Rapid Prototyping Techniques for Tissue Engineering Purposes," *Annals of Medicine*, **40**(4), pp. 268-280.
http://dx.doi.org/10.1080/07853890701881788

Shi, Y., and Zhang, Y., 2008, **"**Simulation of Random Packing of Spherical Particles with Different Size Distributions," *Applied Physics A: Materials Science & Processing,* **92**(3), 621-626.
http://dx.doi.org/10.1007/s00339-008-4547-6

Tan, K.H., Chua, C.K., Leong, K.F., Cheah, C.M., Cheang, P., Abu Bakar, M.S., and Cha, S.W., 2003, "Scaffold Development Using Selective Laser Sintering of Polyetheretherketone-Hydroxyapatite Biocomposite Blends," *Biomaterials*, **24**(18), pp. 3115-3123.
http://dx.doi.org/10.1016/S0142-9612(03)00131-5

Wang, Y., Bergstrom, J., and Burman, C., 2006, "Characterization of an Iron-Based Laser Sintered Material," *Journal of Materials Processing Technology*, **172**(1), pp. 77-87.
http://dx.doi.org/10.1016/j.jmatprotec.2005.09.004

Xiao, B., and Zhang, Y., 2007, "Laser Sintering of Metal Powders on Top of Sintered Layers under Multiple-Line Laser Scanning," *Journal of Physics D: Applied Physics*, **40**(21), 6725-6734.
http://dx.doi.org/10.1088/0022-3727/40/21/036

Xu, X., Prasher, R., and Lofgreen, K., 2007, Ultralow Thermal Conductivity of Nanoparticle Packed Bed," *Applied Physics Letter*, **91**(20), 203113.
http://dx.doi.org/10.1063/1.2814959

Zhang, Y., Faghri, A., Buckley, C.W., and Bergman, T.L., 2000, "Three-Dimensional Sintering of Two-Component Metal Powders with Stationary and Moving Laser Beams," ASME *J. Heat Transfer***,** **122**(1), pp. 150-158.
http://dx.doi.org/10.1115/1.521445